AIMS Molecular Science, 10(3): 213–262.
DOI: 10.3934/molsci.2023015
Received: 25 May 2023
Revised: 27 July 2023
Accepted: 10 September 2023
Published: 25 September 2023

http://www.aimspress.com/journal/Molecular

Research article

Molecular docking and dynamics studies show: Phytochemicals from Papaya leaves extracts as potential inhibitors of SARS–CoV–2 proteins targets and TNF–alpha and alpha thrombin human targets for combating COVID-19

Mohd Shukri Abd Shukor[1] and Mohd Yunus Abd Shukor[2,*]

[1] Snoc International Sdn Bhd, Lot 343, Jalan 7/16 Kawasan Perindustrian Nilai 7, Inland Port, 71800, Negeri Sembilan, Malaysia
[2] Department of Biochemistry, Faculty of Biotechnology and Biomolecular Sciences, University Putra Malaysia, UPM 43400 Serdang, Selangor, Malaysia

* **Correspondence:** Email: mohdyunus@upm.edu.my; Tel: +60397696722; Fax: +60389430913.

Supplementary Figures

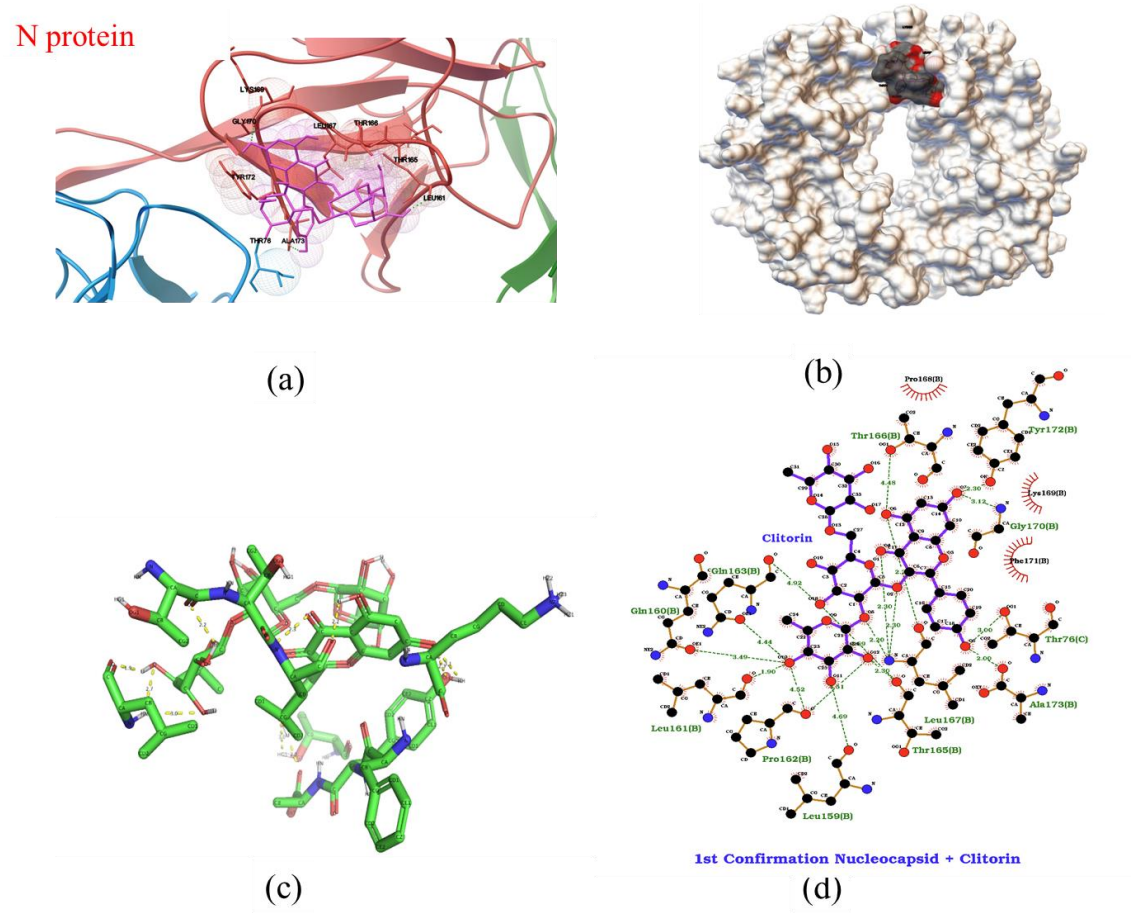

Figure S1. Ribbon diagram of RNA binding domain of nucleocapsid binding to clitorin (a), its three–dimensional representation, where the protein was shown as surface representation in wheat color and ligands shown in stick representation (b), visualization using the pymol software (c) and Ligplot + visualization with the "eyelash" or spoked arc motif denoting hydrophobic contact, while broken green lines denote probable hydrogen bonds, with hydrogen bond lengths indicated in green (d).

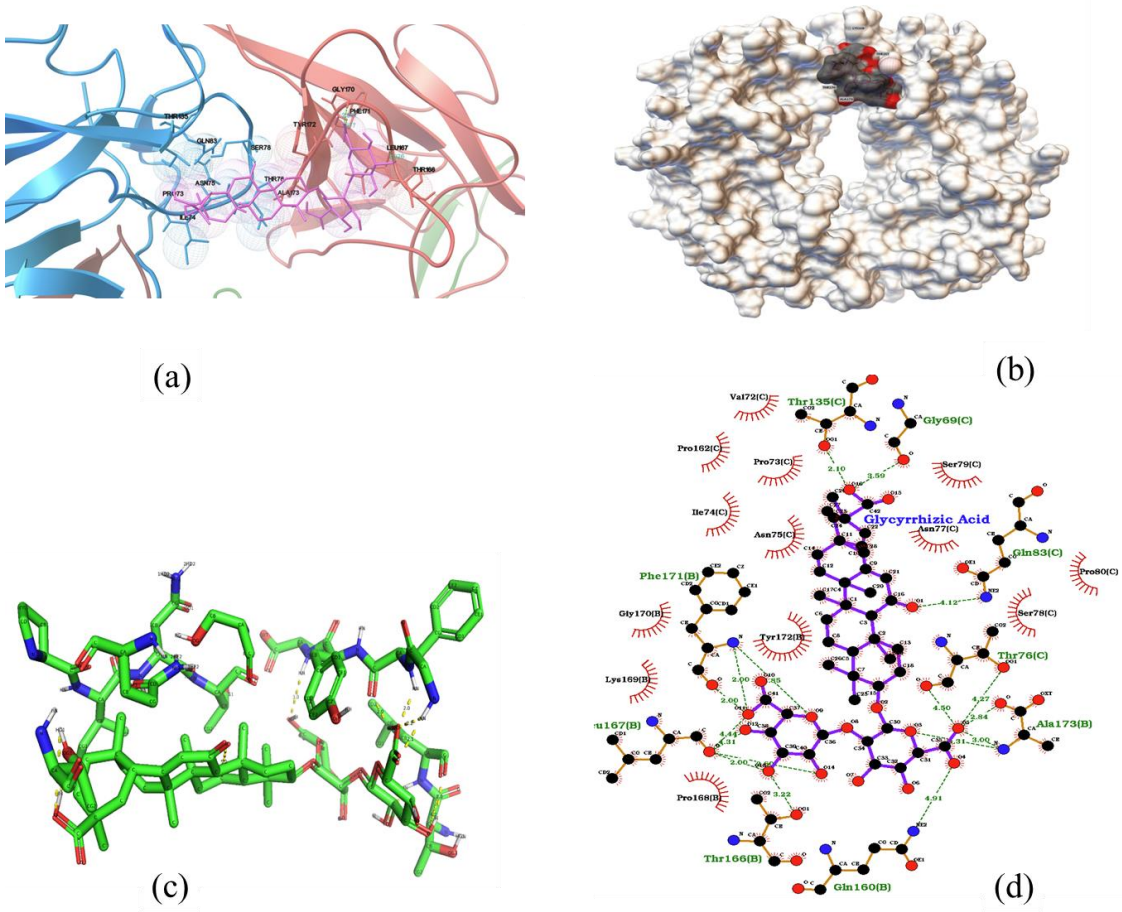

Figure S2. Ribbon diagram of RNA binding domain of nucleocapsid binding to glycyrrhizic acid (a), its three–dimensional representation, where the protein was shown as surface representation in wheat color and ligands shown in stick representation (b), visualization using the pymol software (c) and Ligplot + visualization with the "eyelash" or spoked arc motif denoting hydrophobic contact, while broken green lines denote probable hydrogen bonds, with hydrogen bond lengths indicated in green (d).

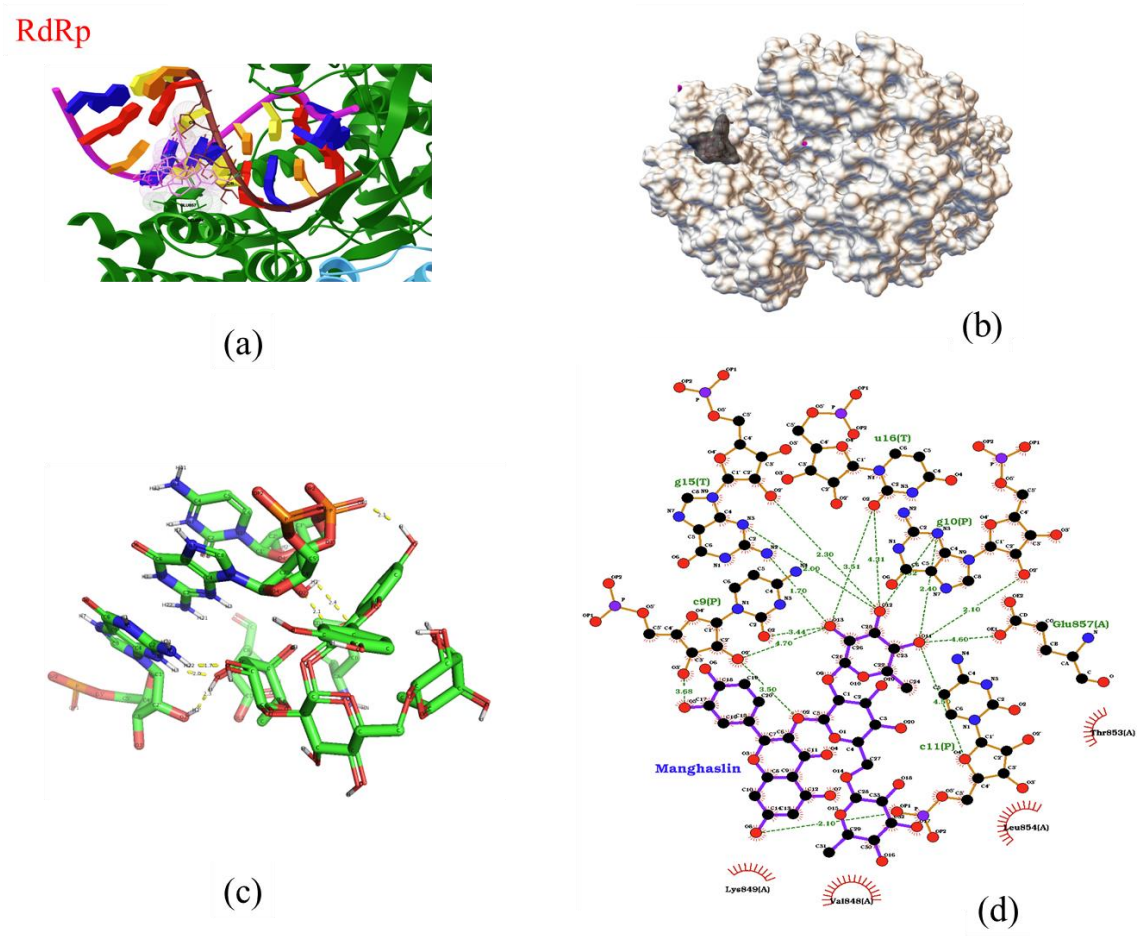

Figure S3. Ribbon diagram of RdRp binding to manghaslin (a), its three–dimensional representation, where the protein was shown as surface representation in wheat color and ligands shown in stick representation (b), visualization using the pymol software (c) and Ligplot + visualization with the "eyelash" or spoked arc motif denoting hydrophobic contact, while broken green lines denote probable hydrogen bonds, with hydrogen bond lengths indicated in green (d).

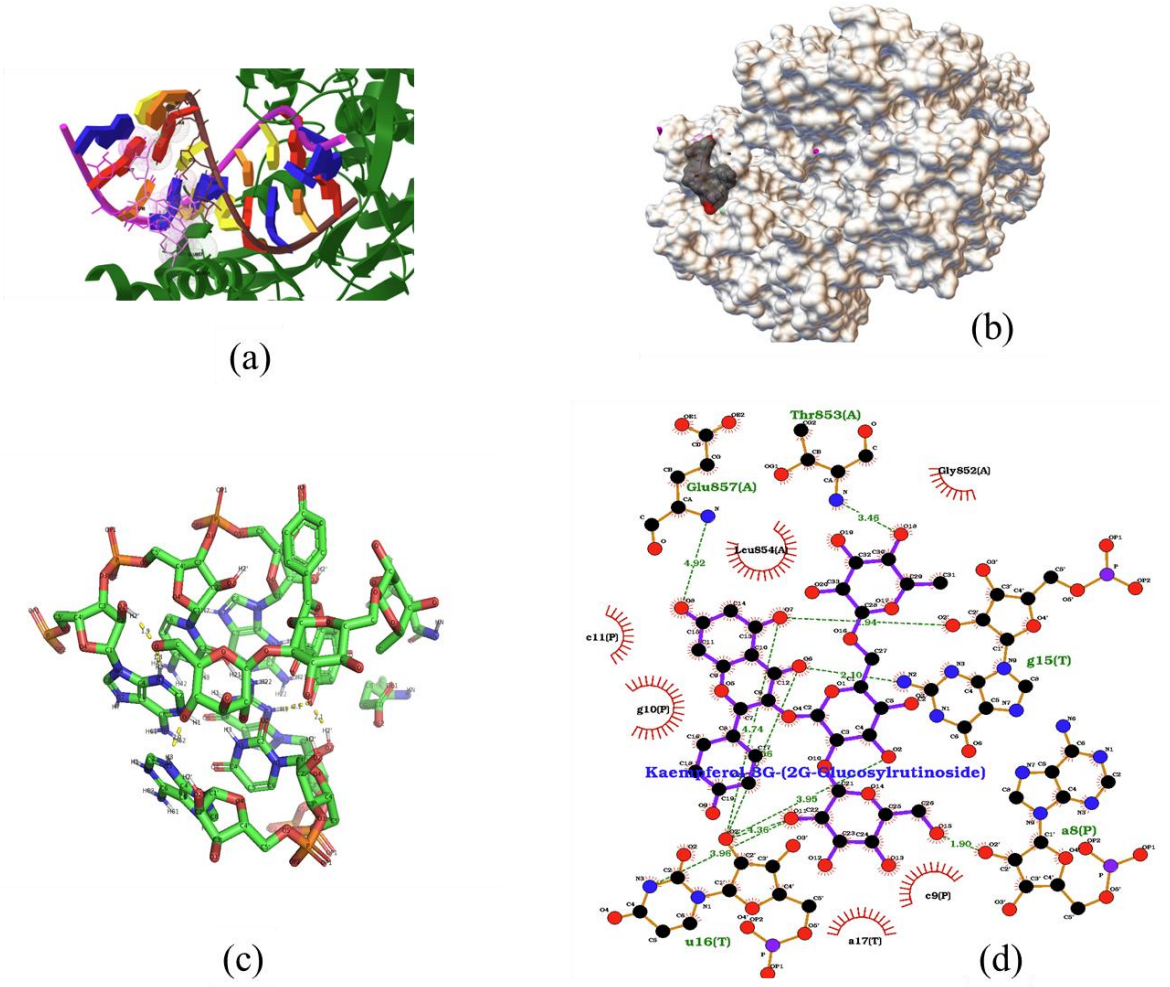

Figure S4. Ribbon diagram of RdRp binding to kaempferol–3–(2G–glucosylrutinoside) (a), its three–dimensional representation, where the protein was shown as surface representation in wheat color and ligands shown in stick representation (b), visualization using the pymol software (c) and Ligplot + visualization with the "eyelash" or spoked arc motif denoting hydrophobic contact, while broken green lines denote probable hydrogen bonds, with hydrogen bond lengths indicated in green (d).

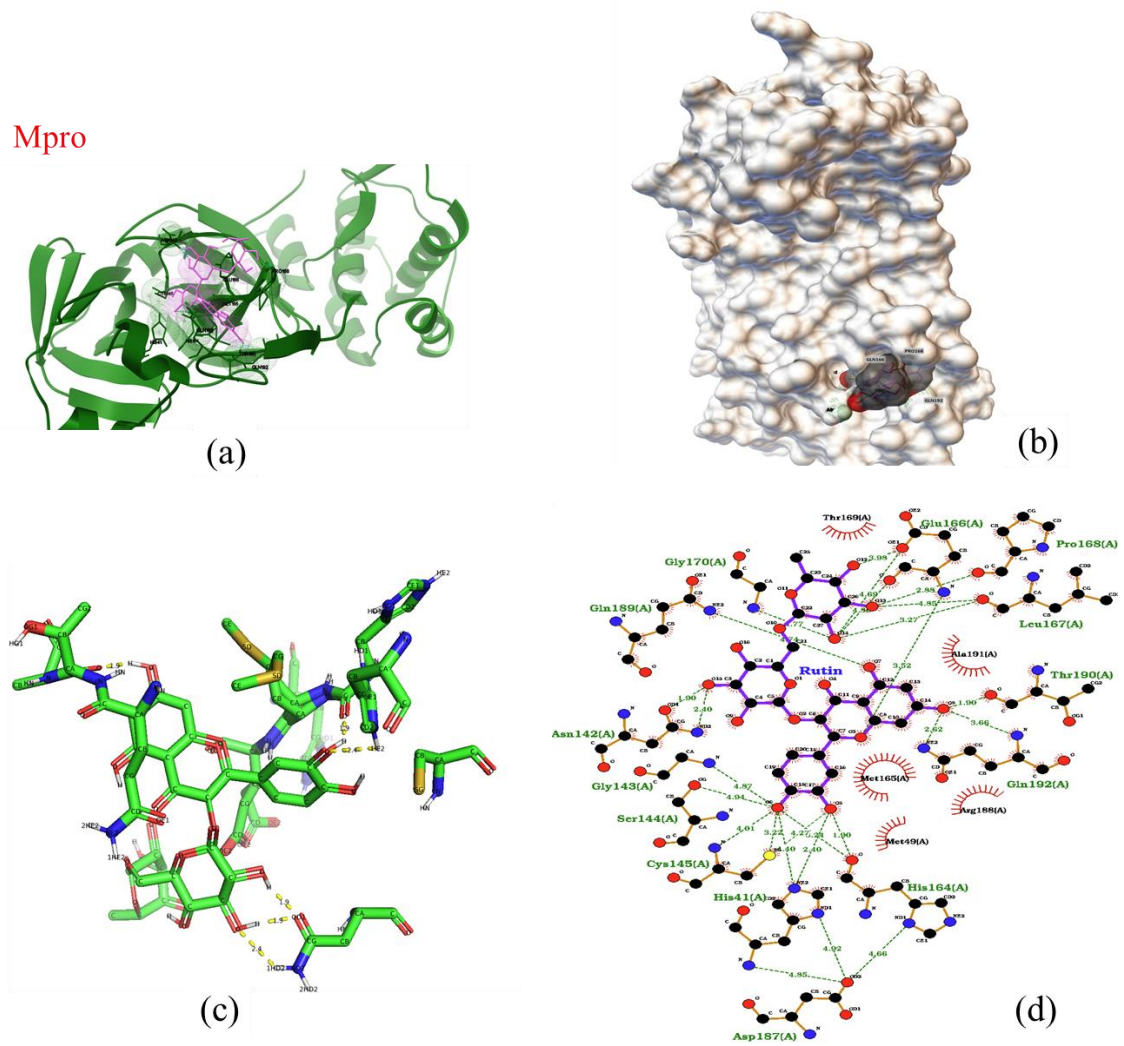

Figure S5. Ribbon diagram of Mpro binding to rutin (a), its three–dimensional representation, where the protein was shown as surface representation in wheat color and ligands shown in stick representation (b), visualization using the pymol software (c) and Ligplot + visualization with the "eyelash" or spoked arc motif denoting hydrophobic contact, while broken green lines denote probable hydrogen bonds, with hydrogen bond lengths indicated in green (d).

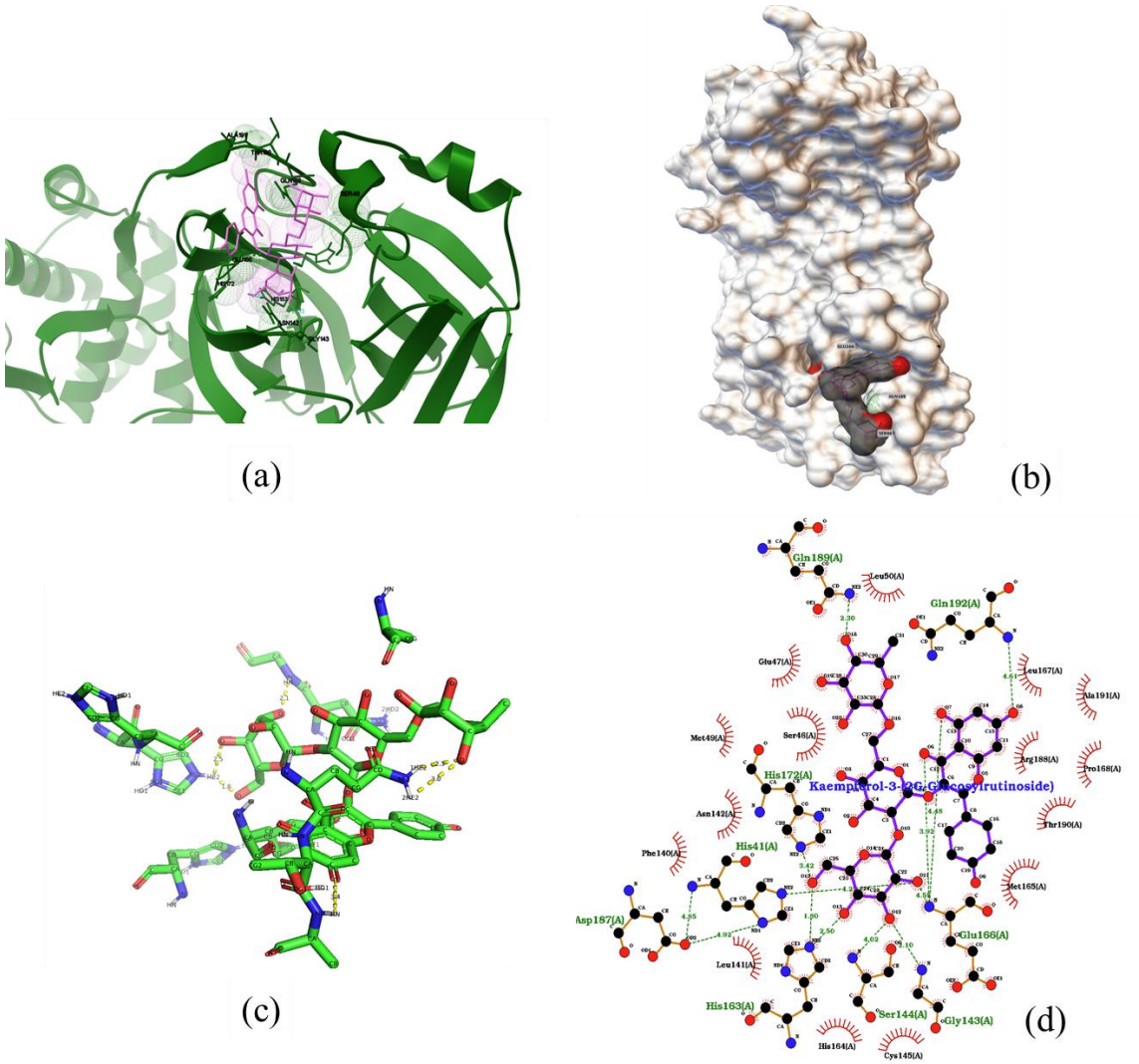

Figure S6. Ribbon diagram of Mpro binding to kaempferol–3–(2G–glucosylrutinoside) (a), its three–dimensional representation, where the protein was shown as surface representation in wheat color and ligands shown in stick representation (b), visualization using the pymol software (c) and Ligplot + visualization with the "eyelash" or spoked arc motif denoting hydrophobic contact, while broken green lines denote probable hydrogen bonds, with hydrogen bond lengths indicated in green (d).

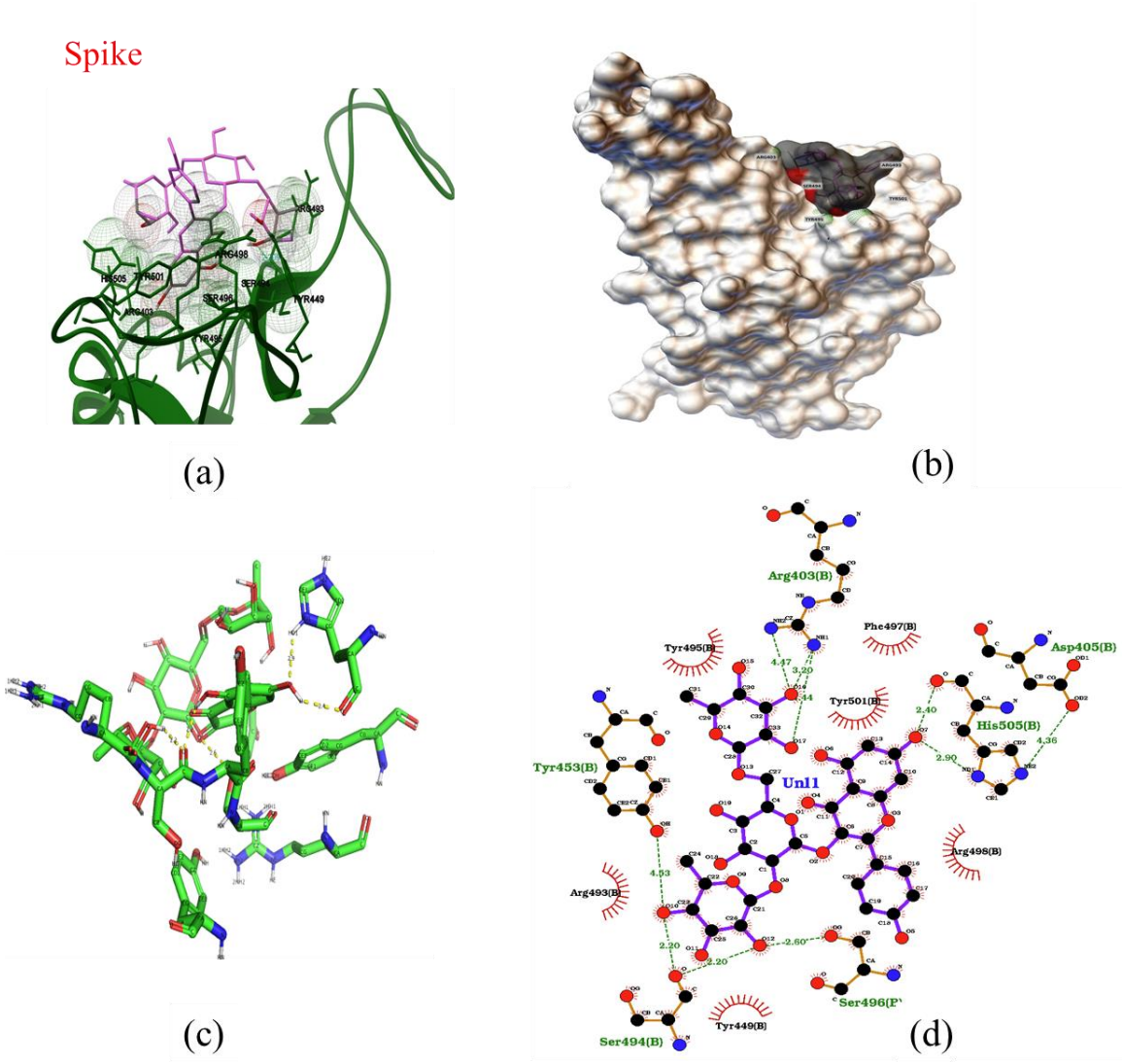

Figure S7. Ribbon diagram of spike protein (Omicron) binding to clitorin (a), its three–dimensional representation, where the protein was shown as surface representation in wheat color and ligands shown in stick representation (b), visualization using the pymol software (c) and Ligplot + visualization with the "eyelash" or spoked arc motif denoting hydrophobic contact, while broken green lines denote probable hydrogen bonds, with hydrogen bond lengths indicated in green (d).

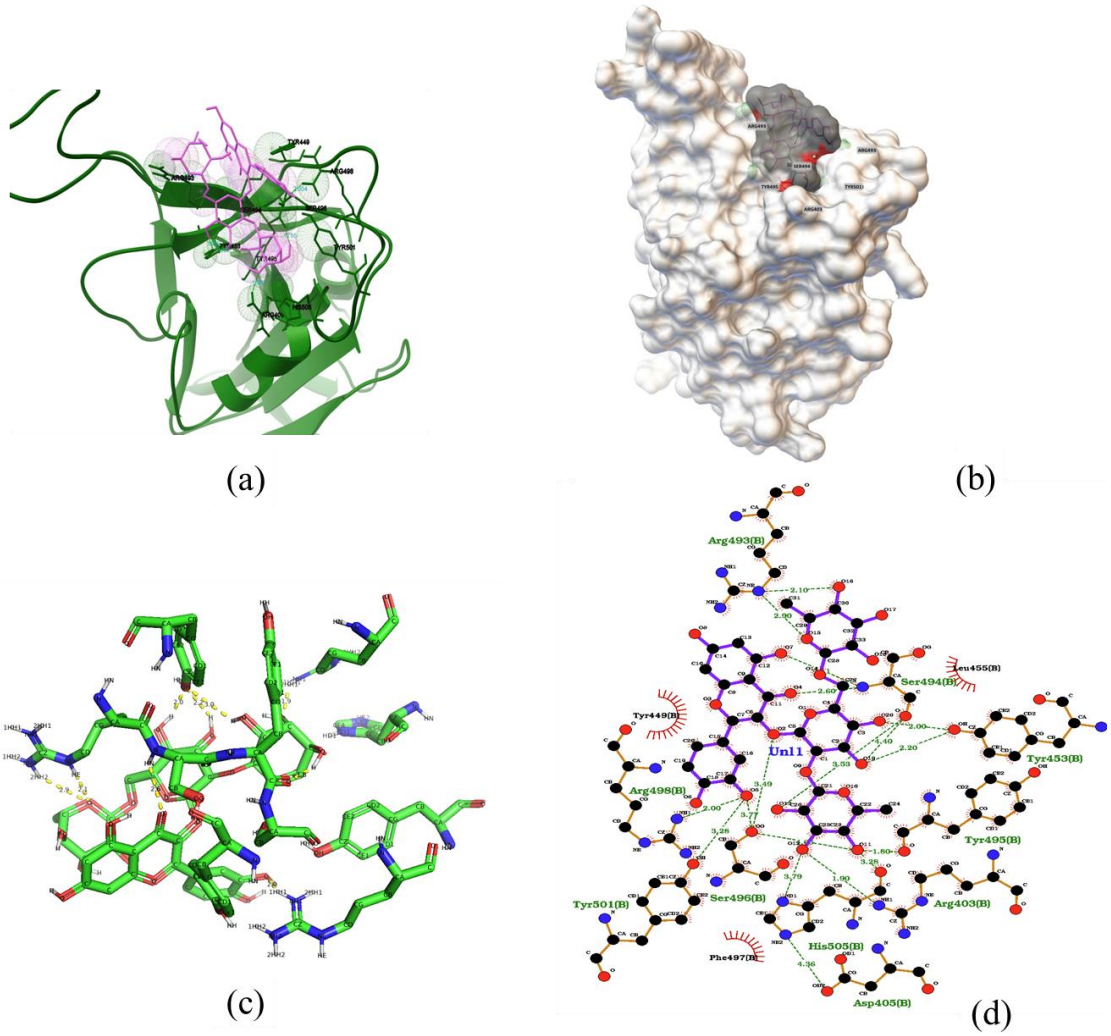

Figure S8. Ribbon diagram of spike protein (Omicron) binding to manghaslin (a), its three–dimensional representation, where the protein was shown as surface representation in wheat color and ligands shown in stick representation (b), visualization using the pymol software (c) and Ligplot + visualization with the "eyelash" or spoked arc motif denoting hydrophobic contact, while broken green lines denote probable hydrogen bonds, with hydrogen bond lengths indicated in green (d).

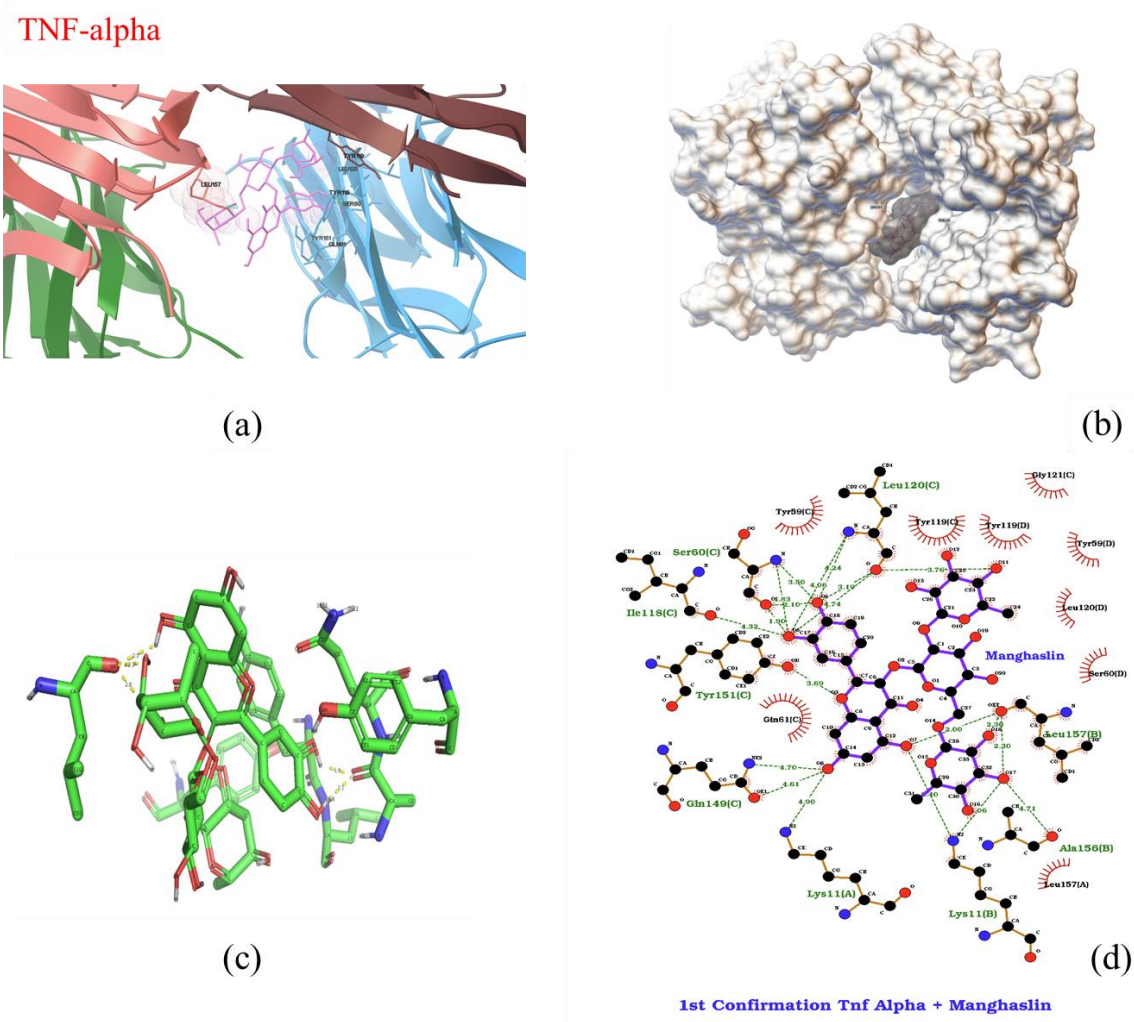

Figure S9. Ribbon diagram of TNF-alpha binding to manghaslin (a), its three–dimensional representation, where the protein was shown as surface representation in wheat color and ligands shown in stick representation (b), visualization using the pymol software (c) and Ligplot + visualization with the "eyelash" or spoked arc motif denoting hydrophobic contact, while broken green lines denote probable hydrogen bonds, with hydrogen bond lengths indicated in green (d).

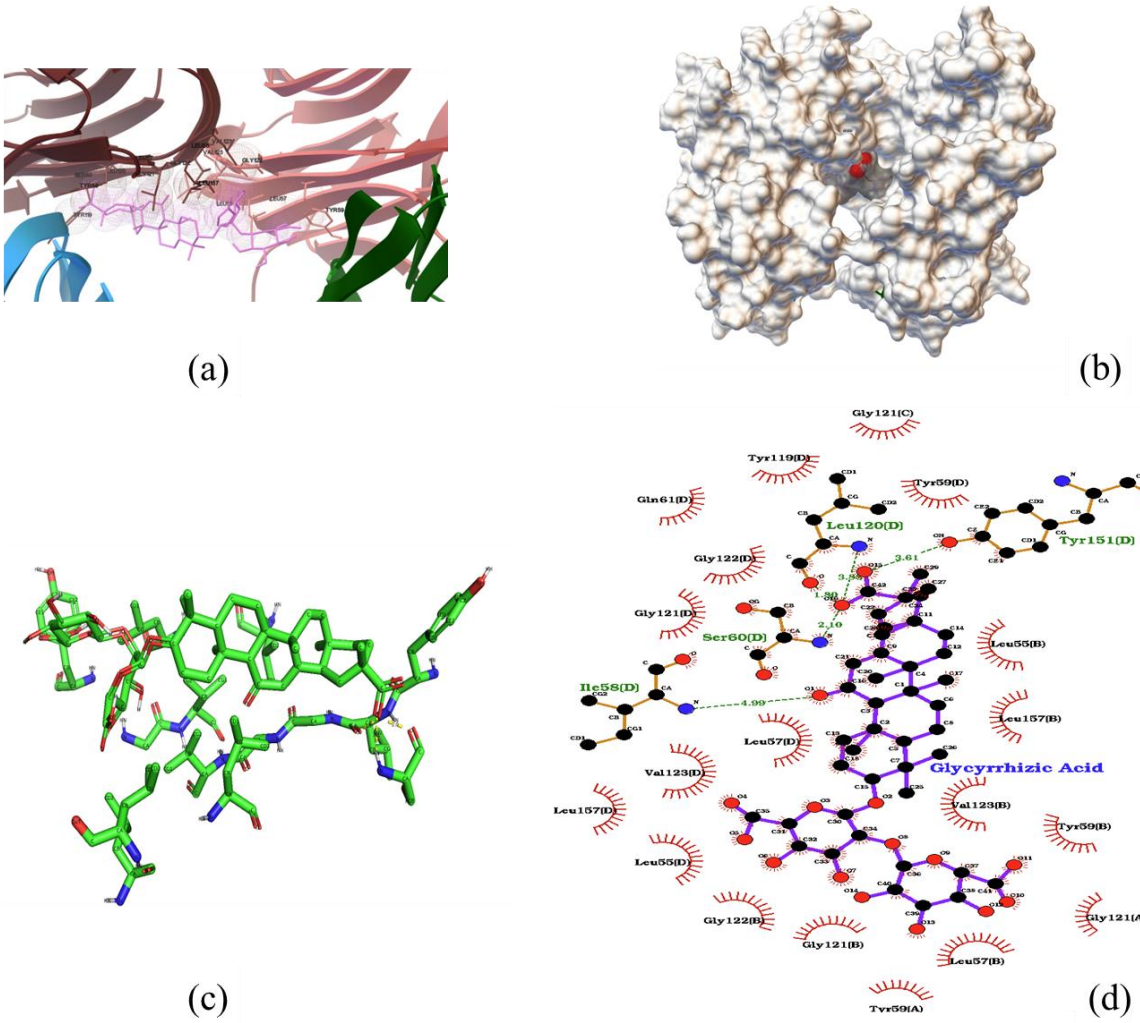

Figure S10. Ribbon diagram of TNF-alpha binding to glycyrrhizic acid (a), its three–dimensional representation, where the protein was shown as surface representation in wheat color and ligands shown in stick representation (b), visualization using the pymol software (c) and Ligplot + visualization with the "eyelash" or spoked arc motif denoting hydrophobic contact, while broken green lines denote probable hydrogen bonds, with hydrogen bond lengths indicated in green (d).

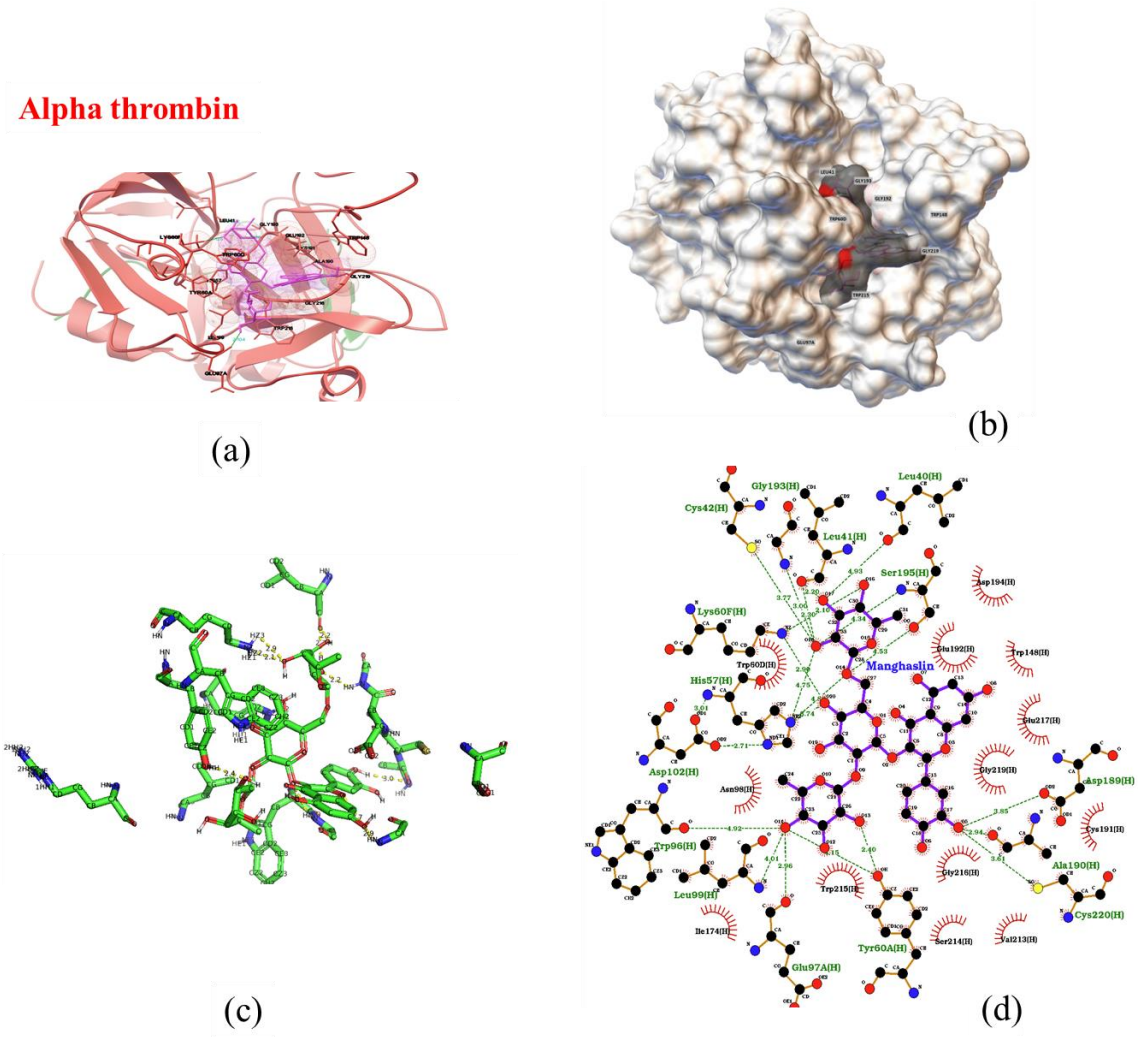

Figure S11. Ribbon diagram of alpha-thrombin binding to manghaslin (a), its three–dimensional representation, where the protein was shown as surface representation in wheat color and ligands shown in stick representation (b), visualization using the pymol software (c) and Ligplot + visualization with the "eyelash" or spoked arc motif denoting hydrophobic contact, while broken green lines denote probable hydrogen bonds, with hydrogen bond lengths indicated in green (d).

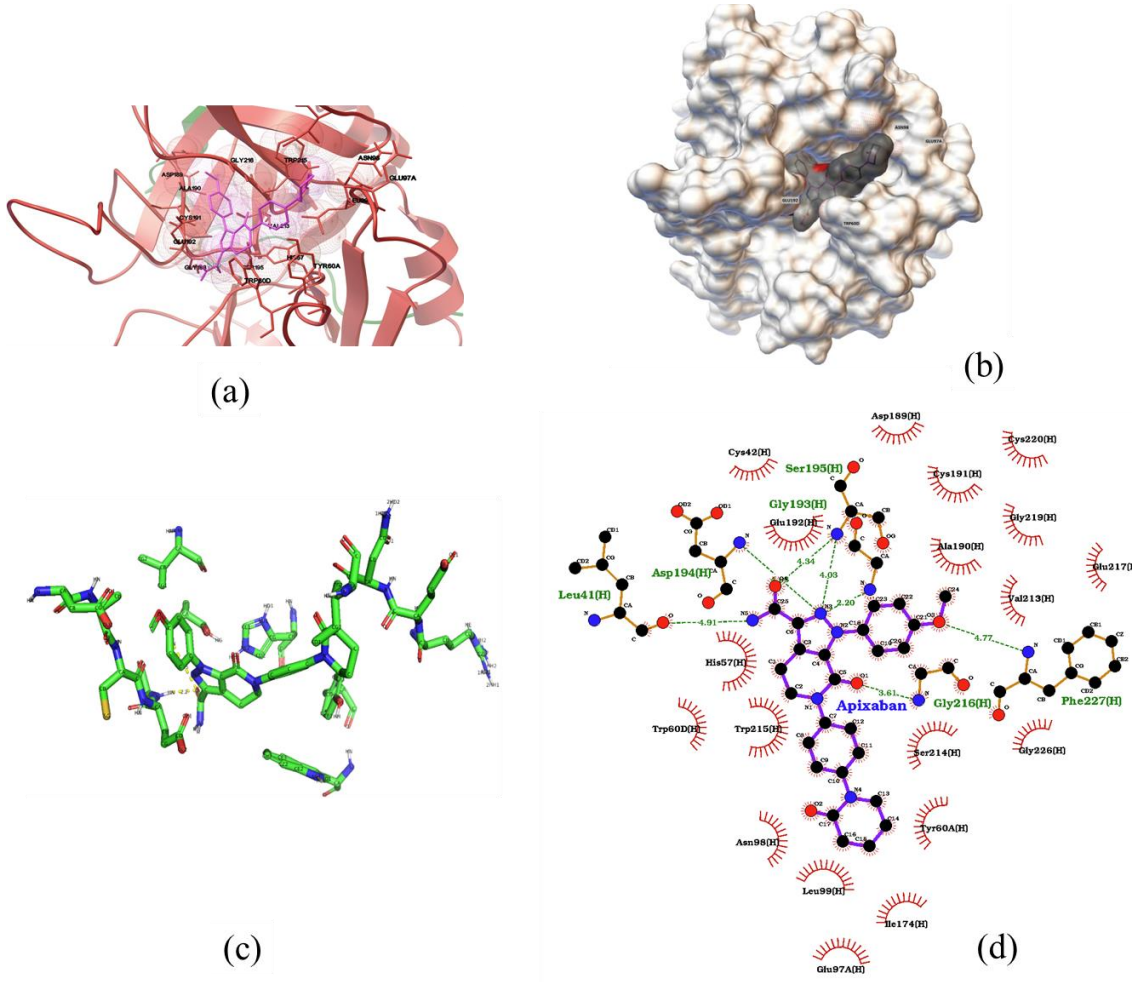

Figure S12. Ribbon diagram of alpha-thrombin binding to apixaban (a), its three–dimensional representation, where the protein was shown as surface representation in wheat color and ligands shown in stick representation (b), visualization using the pymol software (c) and Ligplot + visualization with the "eyelash" or spoked arc motif denoting hydrophobic contact, while broken green lines denote probable hydrogen bonds, with hydrogen bond lengths indicated in green (d).

Supplementary Tables

Table S1. Total binding–free energies and individual energy term (D_{Gtotal} binding ± SD) for the top three compounds binding to TNF alpha.

	Protodioscin (kJ/mol)	Manghaslin (kJ/mol)	Glycyrrhizic acid (kJ/mol)
van der Waal energy	–247.419 ± 14.506	–199.920 ± 17.464	–278.375 ± 17.816
Electrostatic energy	–85.653 ± 26.775	–36.920 ± 20.029	–30.071 ± 12.000
Polar solvation energy	235.621 ± 83.399	189.594 ± 33.503	181.778 ± 22.601
SASA energy	–29.677 ± 1.848	–25.634 ± 1.826	–30.456 ± 1.855
SAV energy	0.000 ± 0.000	0.000 ± 0.000	0.000 ± 0.000
WCA energy	0.000 ± 0.000	0.000 ± 0.000	0.000 ± 0.000
Binding energy	–127.128 ± 77.370	–72.880 ± 16.314	–157.125 ±17.869

Note: solvent–accessible surface area (SASA); Weeks–Chandler–Andersen (WCA); solvent accessible volume (SAV); standard deviation (SD).

Table S2. Total binding–free energies and individual energy term (D_{Gtotal} binding ± SD) for the top three compounds binding to alpha thrombin.

	Protodioscin (kJ/mol)	Manghaslin (kJ/mol)	Apixaban (kJ/mol)
van der Waal energy	–246.698 ± 33.180	–260.956 ± 20.536	–172.537 ± 28.948
Electrostatic energy	–78.100 ± 16.542	–94.185 ± 21.761	–45.665 ± 20.212
Polar solvation energy	286.757 ± 58.816	365.156 ± 31.869	196.161 ± 58.658
SASA energy	–33.777 ± 2.383	–29.874 ± 1.694	–18.181 ± 3.160
SAV energy	0.000 ± 0.000	0.000 ± 0.000	0.000 ± 0.000
WCA energy	0.000 ± 0.000	0.000 ± 0.000	0.000 ± 0.000
Binding energy	–71.818 ± 32.273	–19.860 ± 22.294	–40.221 ± 32.607

Note: solvent–accessible surface area (SASA); Weeks–Chandler–Andersen (WCA); solvent accessible volume (SAV); standard deviation (SD).

Table S3. Total binding–free energies and individual energy term (D_{Gtotal} binding ± SD) for the top three compounds binding to N–protein binding sites.

	Protodioscin (kJ/mol)	Glycyrrhizic acid (kJ/mol)	Clitorin (kJ/mol)
van der Waal energy	–200.040 ± 48.750	–139.538 ± 22.089	–153.925 ± 13.158
Electrostatic energy	–93.656 ± 44.619	–32.312 ± 9.610	–69.552 ± 31.641
Polar solvation energy	259.142 ± 91.560	128.270 ± 25.724	206.863 ± 52.406
SASA energy	–28.295 ± 5.098	–19.207 ± 2.357	–22.316 ± 1.558
SAV energy	0.000 ± 0.000	0.000 ± 0.000	0.000 ± 0.000
WCA energy	0.000 ± 0.000	0.000 ± 0.000	0.000 ± 0.000
Binding energy	–62.850 ± 34.184	–62.787 ± 22.231	–38.930 ± 27.639

Note: solvent–accessible surface area (SASA); Weeks–Chandler–Andersen (WCA); solvent accessible volume (SAV); standard deviation (SD).

Table S4. Total binding–free energies and individual energy term (D_{Gtotal} binding ± SD) for the top three compounds binding to RDRP.

	Protodioscin (kJ/mol)	Manghaslin (kJ/mol)	Kaempferol_3_(2G–glucosylrutinoside (kJ/mol)
van der Waal energy	–122.893 ± 22.199	–101.193 ± 41.814	–37.889 ± 42.778
Electrostatic energy	–30.251 ± 28.964	–22.999 ± 21.426	–18.180 ± 24.410
Polar solvation energy	119.380 ± 48.500	98.751 ± 41.848	54.039 ± 84.695
SASA energy	–17.602 ± 2.404	–13.168 ± 5.837	–5.905 ± 6.930
SAV energy	0.000 ± 0.000	0.000 ± 0.000	0.000 ± 0.000
WCA energy	0.000 ± 0.000	0.000 ± 0.000	0.000 ± 0.000
Binding energy	–51.366 ± 27.185	–38.609 ± 32.825	–7.935 ± 58.853

Note: solvent–accessible surface area (SASA); Weeks–Chandler–Andersen (WCA); solvent accessible volume (SAV); standard deviation (SD).

Table S5. Total binding–free energies and individual energy term (D_{Gtotal} binding ± SD) for the top three compounds binding to MPro.

	Protodioscin (kJ/mol)	Rutin (kJ/mol)	Kaempferol_3_(2G–glucosylrutinoside (kJ/mol)
van der Waal energy	–200.953 ± 24.641	–49.199 ± 44.306	–32.839 ±57.364
Electrostatic energy	–68.759 ± 35.432	–16.907 ± 30.221	–15.985 ±34.892
Polar solvation energy	210.063 ± 53.730	55.508 ± 81.185	82.023 ± 98.322
SASA energy	–26.630 ± 3.818	–6.700 ± 5.434	–4.576 ± 8.220
SAV energy	0.000 ± 0.000	0.000 ± 0.000	0.000 ± 0.000
WCA energy	0.000 ± 0.000	0.000 ± 0.000	0.000 ± 0.000
Binding energy	–86.279 ± 23.891	–17.297 ± 50.752	28.623 ± 37.819

Note: solvent–accessible surface area (SASA); Weeks–Chandler–Andersen (WCA); solvent accessible volume (SAV); standard deviation (SD).

Table S6. Total binding–free energies and individual energy term (D_{Gtotal} binding ± SD) for the top–three compounds binding to Spike proteins (omicron).

	Protodioscin (kJ/mol)	Manghaslin (kJ/mol)	Clitorin (kJ/mol)
van der Waal energy	–138.002 ± 18.715	–108.327 ± 47.049	–92.927 ± 39.730
Electrostattic energy	–74.796 ± 43.068	–37.604 ± 21.527	–26.132 ± 21.549
Polar solvation energy	168.283 ± 58.520	116.949 ± 53.549	95.990 ± 44.414
SASA energy	–18.688 ± 3.036	–12.444 ± 5.405	–11.379 ± 4.121
SAV energy	0.000 ± 0.000	0.000 ± 0.000	0.000 ± 0.000
WCA energy	0.000 ± 0.000	0.000 ± 0.000	0.000 ± 0.000
Binding energy	–63.203 ± 41.170	–41.426 ± 23.587	–34.448 ± 24.049l

Note: solvent–accessible surface area (SASA); Weeks–Chandler–Andersen (WCA); solvent accessible volume (SAV); standard deviation (SD).